

Diversified Arbitrary Style Transfer via Deep Feature Perturbation

Zhizhong Wang, Lei Zhao, Lihong Qiu, Haibo Chen,
Qihang Mo, Sihuan Lin, Wei Xing, Dongming Lu

College of Computer Science and Technology, Zhejiang University
{endywon, cszhl, zjusheldon, feng123, moqihang, linsh, wxing, ldm}@zju.edu.cn

Abstract

Image style transfer is an underdetermined problem, where a large number of solutions can explain the same constraint (i.e., the content and style). Most current methods always produce visually identical outputs, which lack of diversity. Recently, some methods have introduced an alternative diversity loss to train the feed-forward networks for diverse outputs, but they still suffer from many issues. In this paper, we propose a simple yet effective method for diversified style transfer. Our method can produce diverse outputs for arbitrary styles by incorporating the whitening and coloring transforms (WCT) with a novel deep feature perturbation (DFP) operation, which uses an orthogonal random noise matrix to perturb the deep image features while keeping the original style information unchanged. In addition, our method is learning-free and could be easily integrated into many existing WCT-based methods and empower them to generate diverse results. Experimental results demonstrate that our method can greatly increase the diversity while maintaining the quality of stylization. And several new user studies show that users could obtain more satisfactory results through the diversified approaches based on our method.

1 Introduction

The pioneering works of Gatys, Ecker, and Bethge (2015b) have proved the power of deep convolutional neural networks (DCNNs) in style transfer (Gatys, Ecker, and Bethge 2016) and texture synthesis (Gatys, Ecker, and Bethge 2015a), in which the style of an image is represented by the correlations (i.e., Gram matrix) between features extracted by a pre-trained DCNN. Since then, significant efforts have been made to develop this in many aspects including efficiency (Ulyanov et al. 2016; Johnson, Alahi, and Fei-Fei 2016; Li and Wand 2016b), quality (Li and Wand 2016a; Wang et al. 2017; Liao et al. 2017; Gu et al. 2018), generality (Chen et al. 2017; Dumoulin, Shlens, and Kudlur 2017; Huang and Belongie 2017; Li et al. 2017b; Sheng et al. 2018), user control (Champandard 2016; Gatys et al. 2017) and photorealism (Luan et al. 2017; Li et al. 2018), etc. These methods are mainly based on two generative ways: iterative optimization (Gatys, Ecker, and Bethge 2016) or trained feed-forward networks (Ulyanov et al. 2016; Johnson, Alahi, and Fei-Fei 2016). However, for the former, although the initialization may slightly affect the output, the

results are visually identical when it is fixed. For the latter, once trained, they would only produce fixed outputs for the fixed inputs. Therefore, most of the existing style transfer methods have poor capacity to produce diverse outcomes.

As a matter of fact, the Gram-based style transfer is an underdetermined problem, since there could be innumerable solutions that can explain the same Gram matrix. This reveals the ability of the Gram-based approaches to produce diverse results. However, due to the limitations of the aforementioned generative ways, this is a challenging task that has been attracting many efforts. For instance, to address it, Li et al. (2017a) have introduced a diversity loss that penalizes the feature similarities of different samples in a mini-batch. Ulyanov, Vedaldi, and Lempitsky (2017) minimize the Kullback-Leibler divergence between the generated distribution and a quasi-uniform distribution on the Julesz ensemble (Julesz 1981; Zhu, Liu, and Wu 2000). Their methods could generate diverse texture samples or stylized images to a certain extent, but the feed-forward networks have to be trained for every style, which is not generalized for arbitrary styles. Besides, since the quality of stylization depends heavily on the weight of the diversity loss, the network is hard to train and the degree of diversity is limited as well. Moreover, these techniques cannot be simply integrated into recent arbitrary style transfer methods (Li et al. 2017b; Sheng et al. 2018; Li et al. 2018) as these methods transfer arbitrary styles in a style-agnostic manner.

To address these limitations, we rethink the problem of diversity and an important insight has been reached is that if we can obtain different image features with the same Gram matrix, then the diverse results can be obtained. Obviously, the problem of diversity has now been transformed into the problem of how to obtain the different image features with the same Gram matrix. Fortunately, we find that the work of Li et al. (2017b) can give us some inspiration as it splits the Gram matrix by matrix decomposition, and separates the matching of Gram matrix by several feature transforms, i.e., the whitening and coloring transforms (WCT).

Based on the above analyses, we propose a simple yet effective method, i.e., deep feature perturbation (DFP), and incorporate it into WCT (Li et al. 2017b), to achieve diversified arbitrary style transfer. Our diversity is achieved by using an orthogonal noise matrix to perturb the image features extracted by a DCNN while keeping the original style in-

formation unchanged. That is to say, although the perturbed features may be different from each other, they all have the same Gram matrix. For ease of understanding, we regard Gram matrix as the style of an image, and define that different images with the same Gram matrix share the same style-specific image space.

In this work, since our deep feature perturbation is based on the framework of WCT (Li et al. 2017b), it can be easily incorporated into many WCT-based methods (Sheng et al. 2018; Li et al. 2018) and empower them to generate diverse results without any extra learning process. Note that this learning-free process is fundamentally different from the aforementioned diversity techniques that require learning with pre-defined styles. Therefore, our method is able to achieve diversified arbitrary style transfer.

The main contributions of this work are threefold:

We propose to use deep feature perturbation, i.e., perturbing the deep features by orthogonal noise matrix while keeping the original style information unchanged, to achieve diversified arbitrary style transfer.

Our method can be easily incorporated into existing WCT-based methods (Li et al. 2017b; Sheng et al. 2018; Li et al. 2018) which are used for different style transfer tasks, e.g., artistic style transfer, semantic-level style transfer and photo-realistic style transfer.

We demonstrate the effectiveness of our method from both qualitative and quantitative aspects, and conduct several new user studies to justify our superiority.

2 Related Work

Gram-based Methods. Gatys, Ecker, and Bethge (Gatys, Ecker, and Bethge 2015b; 2015a; 2016) proposed an algorithm for arbitrary style transfer and texture synthesis based on matching the correlations (i.e., Gram matrix) between deep features extracted by a pre-trained DCNN within an iterative optimization framework. But one of the major drawbacks is the inefficiency. To address this, (Johnson, Alahi, and Fei-Fei 2016) and (Ulyanov et al. 2016; Ulyanov, Vedaldi, and Lempitsky 2017) directly trained feed-forward generative networks for fast style transfer. But these methods need to retrain the network every time for a new style, which is inflexible. For this limitation, some methods (Dumoulin, Shlens, and Kudlur 2017; Zhang and Dana 2018; Chen et al. 2017; Li et al. 2017a) were proposed to incorporate multiple styles into one single network, but they are still limited in a fixed number of pre-defined styles. More recently, (Huang and Belongie 2017) further allowed arbitrary style transfer in one single feed-forward network.

WCT-based Methods. Recently, (Li et al. 2017b) have proposed to exploit a series of feature transforms to achieve fast arbitrary style transfer in a style learning-free manner. Their feed-forward network is only trained on the image reconstruction task. And the transfer task is formulated as an image reconstruction process, with the features of the content image being *whitened* at intermediate layers with regard to their style statistics (i.e., Gram matrix), and then *colored* to exhibit the same statistical characteristics of the style image. This method is essentially a Gram-based method, but it

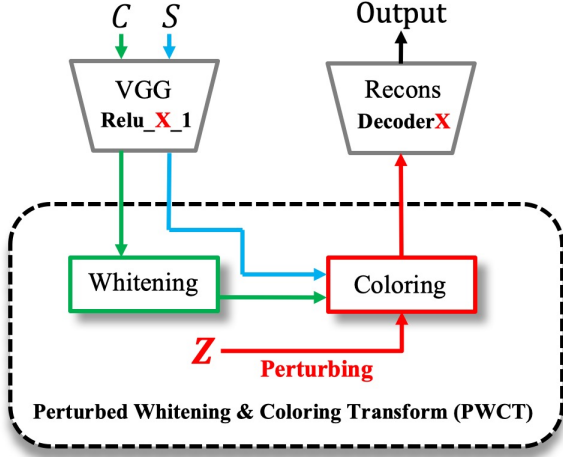
splits the Gram matrix by matrix decomposition, and separates the matching of Gram matrix by whitening and coloring transforms (WCT), thus providing an opportunity for our deep feature perturbation. Furthermore, Sheng et al. (2018) combined it with style swap (Chen and Schmidt 2016) for higher quality semantic-level style transfer, and Li et al. (2018) developed this to fast photo-realistic style transfer. More recently, Li et al. (2019) derived the form of transformation matrix theoretically and directly learned it with a feed-forward network. Except for the last one, since these methods are based on the learning-free WCT process, our deep feature perturbation can be easily integrated into them and empower them to generate diverse results, which will be shown in Section 5.

Diversified Methods. Our method is closely related to (Li et al. 2017a) and (Ulyanov, Vedaldi, and Lempitsky 2017). Li et al. (2017a) introduced a diversity loss to allow the network to generate diverse outputs. It explicitly measures the variations in visual appearances between the generated results under the same texture but different input noise, and penalizes them in a mini-batch. Ulyanov, Vedaldi, and Lempitsky (2017) proposed a new formulation that allowed to train generative networks which sampled the Julesz ensemble (Julesz 1981; Zhu, Liu, and Wu 2000), this could help generate images with high visual fidelity as well as high diversity. Specifically, the diversity term of its learning objective is similar to that of Li et al. (2017a), which quantifies the lack of diversity in the batch by mutually comparing the generated images. Although their methods could generate diverse outputs to a certain extent, there are three main shortcomings. (1) Diversity is not for arbitrary styles. The feed-forward networks have to be trained for every style, which is inflexible. (2) Network is hard to train. The weight of diversity term has to be fine-tuned for different styles, and we cannot know the results until the network training has completed. Once the value of weight is too high, it will seriously affect the quality of stylization. (3) Since the diversity is learned by penalizing the variations in the batch and the weight of diversity term could not be too high, the degree of diversity is limited.

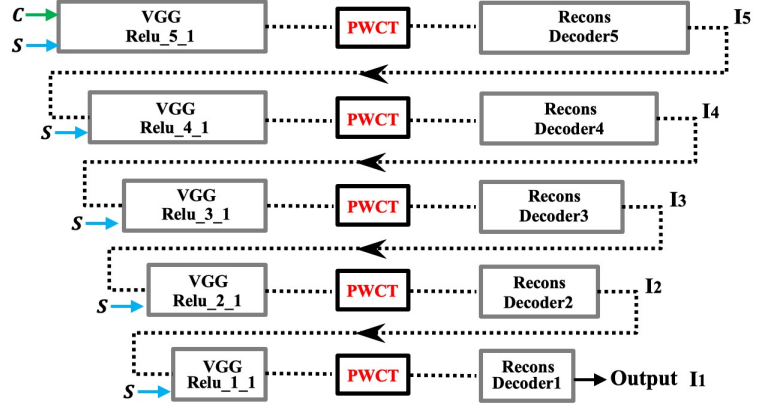
Our method is based on WCT, but empowers it to generate diverse results. Being different from recent diversified methods (Li et al. 2017a; Ulyanov, Vedaldi, and Lempitsky 2017), our diversity is suitable for arbitrary styles. And since the transfer process of ours is learning-free, it is much easier to find the trade-off between diversity and quality. Moreover, without any extra constraints, our method can theoretically produce infinite number of satisfactory solutions.

3 Style-Specific Image Space

Defining the style of an image is a quite tricky problem, and so far no unified conclusion has been reached. Informally, a style can be regarded as a family of visual attributes, such as color, brush strokes and line drawing, etc. Recently, Gatys, Ecker, and Bethge (Gatys, Ecker, and Bethge 2015b; 2015a; 2016) have proposed a new style representation (Gram matrix) for artistic images. In their works, the style of an image is represented by the correlations between deep features extracted by a pre-trained DCNN. Given an image \vec{x} as input,



(a) Single-level stylization



(b) Multi-level stylization

Figure 1: Diversified arbitrary style transfer pipeline. (a) We add an orthogonal noise matrix Z to perturb the whitening and coloring transform. Like (Li et al. 2017b), the VGG and DecoderX are first trained for image reconstruction and then fixed for style transfer. C and S denote the content image and style image, respectively. (b) Our perturbed whitening and coloring transform can be applied in every level of the multi-level stylization framework in (Li et al. 2017b).

the vectorized feature map extracted from a certain layer (we only take one layer as an example) of the VGG model (Simonyan and Zisserman 2014) is denoted as $F \in \mathbb{R}^{C \times HW}$, where H, W are the height and width of the feature, and C is the number of channels. The style of the image \tilde{x} can be represented as follows:

$$G_{ij} = \sum_k F_{ik} F_{jk} = FF^T \in \mathbb{R}^{C \times C}, \quad (1)$$

where F_{ik} and F_{jk} are the activations of the i^{th} and j^{th} filter at position k , F^T is the transpose matrix of F .

It is obvious that, for a definite Gram matrix \mathcal{G} , there could be a large number of feature maps corresponding to it. Let $\Phi(\tilde{x})$ denote the vectorized feature of an image \tilde{x} in layer Φ . The image is perceived as the style \mathcal{G} if the Gram matrix of its deep feature matches \mathcal{G} . Formally, given the loss function:

$$\mathcal{L}_{\mathcal{G}}(\tilde{x}) = \|\Phi(\tilde{x})\Phi(\tilde{x})^T - \mathcal{G}\|, \quad (2)$$

we define the images that satisfy the following constraint belong to the same style-specific image space of \mathcal{G} .

$$\mathcal{S}_{\mathcal{G}} = \{\tilde{x} \in \mathcal{X} : \mathcal{L}_{\mathcal{G}}(\tilde{x}) = 0\}, \quad (3)$$

where \mathcal{X} is an image set. Images belonging to the same style-specific image space \mathcal{S} are perceptually equivalent.

In particular, sometimes we do not need their Gram matrices to be exactly equal, then we can get the relaxed constraint,

$$\mathcal{S}_{\mathcal{G}}^{\epsilon} = \{\tilde{x} \in \mathcal{X} : \mathcal{L}_{\mathcal{G}}(\tilde{x}) \leq \epsilon\}, \quad (4)$$

in which the images are approximately equivalent in visual perception.

In this work, our deep feature perturbation can easily achieve the first constraint (Eq. 3), while the methods (Li et al. 2017a; Ulyanov, Vedaldi, and Lempitsky 2017) only

satisfy the second constraint (Eq. 4). That is to say, the Gram matrices of the diverse stylized results obtained by our method can be completely equal.

4 Deep Feature Perturbation

Our deep feature perturbation (DFP) is based on the work of Li et al. (2017b) and incorporated into its whitening and coloring transforms, to help produce diverse stylized results. The pipeline is shown in Fig. 1, where the diversified style transfer is mainly achieved by the perturbed whitening and coloring transform (PWCT), which consists of two steps, i.e., whitening transform and perturbed coloring transform.

Whitening Transform. Given a pair of content image I_c and style image I_s , we first extract their vectorized VGG feature maps $F_c = \Phi(I_c) \in \mathbb{R}^{C \times H_c W_c}$ and $F_s = \Phi(I_s) \in \mathbb{R}^{C \times H_s W_s}$ at a certain layer Φ (e.g., *Relu_3_1*), where H_c, W_c (H_s, W_s) are the height and width of the content (style) feature, and C is the number of channels. We first center F_c by subtracting its mean vector m_c . Then the whitening transform (Eq. 5) is used to transform F_c to \hat{F}_c , in which the feature maps are uncorrelated from each other (i.e., $\hat{F}_c \hat{F}_c^T = I$).

$$\hat{F}_c = E_c D_c^{-\frac{1}{2}} E_c^T F_c, \quad (5)$$

where D_c and E_c are obtained by the singular value decomposition (SVD) of the Gram matrix $F_c F_c^T \in \mathbb{R}^{C \times C}$ (Eq. 1), i.e., $F_c F_c^T = E_c D_c E_c^T$. D_c is the diagonal matrix of the eigenvalues, and E_c is the corresponding orthogonal matrix of eigenvectors.

Perturbed Coloring Transform. We first center F_s by subtracting its mean vector m_s . The coloring transform used in (Li et al. 2017b) is essentially the inverse of the whitening step, i.e., using Eq. (6) to transform \hat{F}_c so that we can

Table 1: Quantitative comparisons between single-level perturbation and multi-level perturbation in terms of run-time, tested on images of size 512×512 and a 6GB Nvidia 980Ti GPU.

Fig. 2	(Li et al. 2017b)	I5	I4	I3	I2	I1	I5+I4	I5+I1	I3+I2+I1	I5+I4+I3+I2+I1
Time/sec	3.01	3.53	3.51	3.04	3.03	3.02	4.14	3.54	3.05	4.15
Fig. 3	(Li et al. 2018)	-	I4	I3	I2	I1	I4+I3	I4+I1	I2+I1	I4+I3+I2+I1
Time/sec	0.29	-	0.32	0.31	0.30	0.29	0.33	0.32	0.30	0.34

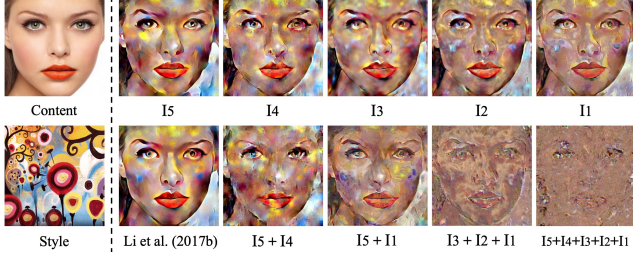


Figure 2: Single-level perturbation vs. Multi-level perturbation. Our DFP is integrated into method (Li et al. 2017b). The top row shows results obtained by only perturbing a single-level stylization in Fig. 1(b). The bottom row shows results obtained by perturbing stylizations in multiple levels.

obtain \hat{F}_{cs}^T which satisfies the same Gram matrix of F_s (i.e., $\hat{F}_{cs}\hat{F}_{cs}^T = F_s F_s^T$).

$$\hat{F}_{cs} = E_s D_s^{\frac{1}{2}} E_s^T \hat{F}_c, \quad (6)$$

where D_s and E_s are obtained by the SVD of the Gram matrix $F_s F_s^T \in \mathbb{R}^{C \times C}$, i.e., $F_s F_s^T = E_s D_s E_s^T$. D_s is the diagonal matrix of the eigenvalues, and E_s is the corresponding orthogonal matrix of eigenvectors.

The goal of coloring transform is to make the Gram matrix of \hat{F}_{cs} the same as that of F_s . According to our analyses in Section 3, the images reconstructed from them share the same style-specific image space. In theory, \hat{F}_{cs} should have a large number of possibilities, but Eq. (6) only produces one of them. In order to traverse these solutions as much as possible, we propose to use deep feature perturbation.

The key idea of our deep feature perturbation is incorporating an orthogonal noise matrix into Eq. (6) to perturb the feature \hat{F}_{cs} while preserving its Gram matrix. Obviously, there are three places to insert the noise matrix, i.e., between $D_s^{\frac{1}{2}}$ and E_s^T , between E_s^T and \hat{F}_c , and on the right side of \hat{F}_c (since $E_s^T E_s = I$ and $\hat{F}_c \hat{F}_c^T = I$). We eventually insert the orthogonal noise matrix between $D_s^{\frac{1}{2}}$ and E_s^T as this may consume the least computation and run-time (we will discuss this in Section 5.2).

We first obtain a random noise matrix (e.g., Gaussian noise matrix) according to the shape of $D_s^{\frac{1}{2}}$ and E_s^T . Assume that the shape of $D_s^{\frac{1}{2}}$ is $(C-k) \times (C-k)$, where k is the number of small singular values (e.g., less than 10^{-5} , Li et

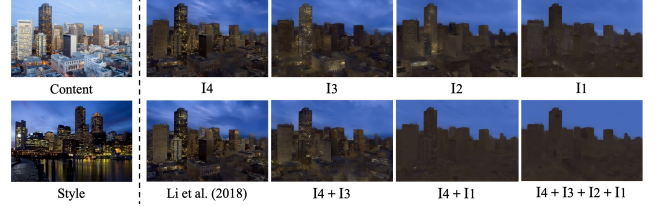


Figure 3: Another comparison of Single-level and Multi-level perturbation. Our DFP is integrated into method (Li et al. 2018). This method only uses four-level stylizations. The top row shows results obtained by only perturbing a single-level stylization. The bottom row shows results obtained by perturbing stylizations in multiple levels.

al. (2017b) suggest removing these small singular values for higher quality results), and the shape of E_s^T is $(C-k) \times C$, then the shape of random noise matrix N is $(C-k) \times (C-k)$. To obtain orthogonal noise matrix, we apply the SVD to decompose N , i.e., $N = E_n D_n V_n^T$, and directly use the orthogonal matrix $Z = E_n \in \mathbb{R}^{(C-k) \times (C-k)}$. Finally, we insert Z between $D_s^{\frac{1}{2}}$ and E_s^T of Eq. (6). Our new perturbed coloring transform is formulated as follows:

$$\hat{F}_{csn} = E_s D_s^{\frac{1}{2}} Z E_s^T \hat{F}_c, \quad (7)$$

since $Z Z^T = I$, we can deduce as follows:

$$\begin{aligned} \hat{F}_{csn} \hat{F}_{csn}^T &= (E_s D_s^{\frac{1}{2}} Z E_s^T \hat{F}_c) (\hat{F}_c^T E_s Z^T D_s^{\frac{1}{2}} E_s^T) \\ &= E_s D_s^{\frac{1}{2}} (Z E_s^T \hat{F}_c \hat{F}_c^T E_s Z^T) D_s^{\frac{1}{2}} E_s^T \\ &= E_s D_s E_s^T = F_s F_s^T \end{aligned}$$

In our later experiments, we find that only using our perturbed coloring transform may reduce the quality of stylization in some methods (e.g., (Sheng et al. 2018)). So we introduce a diversity hyperparameter λ to provide user controls on the trade-off between diversity and quality.

$$\hat{F}_{csn} = \lambda \hat{F}_{csn} + (1 - \lambda) \hat{F}_{cs}. \quad (8)$$

Then, we re-center the \hat{F}_{csn} with the mean vector m_s of the style, i.e., $\hat{F}_{csn} = \hat{F}_{csn} + m_s$. At last, we blend \hat{F}_{csn} with the content feature F_c before feeding it to the decoder.

$$\hat{F}_{csn} = \alpha \hat{F}_{csn} + (1 - \alpha) F_c, \quad (9)$$

where the hyperparameter α serves as the style weight for users to control the transfer effect.

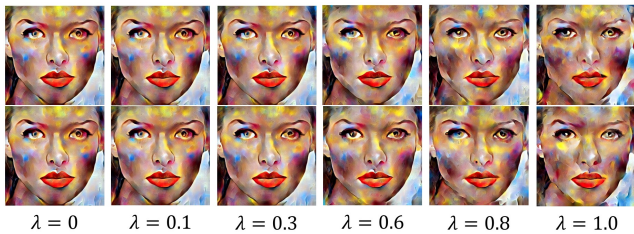


Figure 4: Trade-off between diversity and quality by varying diversity hyperparameter λ . These images are obtained by method (Li et al. 2017b) (+ our DFP).

Multi-level Stylization. We follow the multi-level coarse-to-fine stylization used in (Li et al. 2017b), but replace their WCTs with our PWCTs, as shown in Fig. 1 (b). In fact, we do not need to add noise to every level. We will discuss this in Section 5.2.

Discussions. As a matter of fact, optimizing the diversity loss of (Li et al. 2017a; Ulyanov, Vedaldi, and Lempitsky 2017) can be viewed as a sub-optimal approximation of our method. But since it is only optimized on small batches of a limited dataset, the degree of diversity is limited. By contrast, the number of different orthogonal noise matrices can be infinite, so there could be endless possibilities for the results of our approach. Moreover, our method is learning-free and can be effective for arbitrary styles, while the diversity loss needs to be optimized every time for every style.

5 Experimental Results

5.1 Implementation Details

We incorporate our deep feature perturbation into three existing WCT-based methods which are used for different style transfer tasks, i.e., (Li et al. 2017b) for artistic style transfer, (Sheng et al. 2018) for semantic-level style transfer and (Li et al. 2018) for photo-realistic style transfer. Except for replacing the WCTs with our PWCTs, we do not modify anything else, such as pre-trained models, pre-processing or post-processing operations, etc. In all experiments, the stylization weight α of our diversified versions is consistent with the original versions. We fine-tune the diversity hyperparameter λ to make our quality similar to previous works.

5.2 Ablation Study

Single-level Perturbation versus Multi-level Perturbation. We study the effects of single-level perturbation and multi-level perturbation on two WCT-based methods (Li et al. 2017b; 2018), since they both use the multi-level stylization (while the method (Sheng et al. 2018) only uses a single-level stylization). To perturb only specific levels, we set the diversity hyperparameter λ to 1 for them, and 0 for others. As shown in the top row of Fig. 2, when we perturb separately from the deepest level (I5) to the shallowest level (I1), the quality decreases accordingly. This phenomenon exists in the top row of Fig. 3 as well. We analyze the reason may be that the deeper level stylizes more low-frequency coarse characteristics while the shallower level

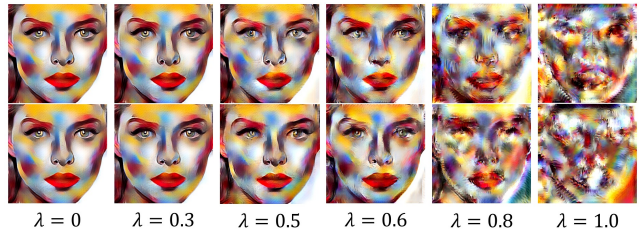


Figure 5: Trade-off between diversity and quality by varying diversity hyperparameter λ . These images are obtained by method (Sheng et al. 2018) (+ our DFP).

stylizes more high-frequency fine characteristics, so adding noise into the shallower levels will directly affect the pixel performance of the final images. Perturbing at the deepest level can achieve comparable stylization quality as the original (see I5 in Fig. 2 and I4 in Fig. 3). On the other hand, multi-level perturbation introduces noise into multiple levels, as shown in the bottom rows of Fig. 2 and Fig. 3. We can see that introducing too much noise will reduce the quality of stylization. We also compare the run-time in Table 1. Note that for method (Li et al. 2018), we only compare the stylization time. Compared with the original methods (column 2), the incremental run-time decreases when we perturb the shallower levels. Nevertheless, the deepest-level perturbation only increases a very small amount of time (in **bold**).

Trade-off between Diversity and Quality. In Eq. (8), we introduce a diversity hyperparameter λ to provide user controls on the trade-off between diversity and quality. In fact, fine-tuning is not necessary for most methods. As we stated earlier (Fig. 2 and Fig. 3), when we perturb only the deepest level (I5 or I4), the results are almost without loss of quality even with the maximum λ value. To demonstrate this more clearly, we compare the effects of different λ values in Fig. 4. For this case, we only perturb the deepest level (I5) for method (Li et al. 2017b). As we can see, the degree of diversity rises with the increase of λ value, while the loss of quality is fairly small. We think this should be attributed to the multi-level stylization and deepest-level perturbation. However, for method (Sheng et al. 2018), since the WCT stylization is only used in a single level, at this point we need to fine-tune the value of λ . As shown in Fig. 5, higher λ value can increase the diversity, but at the same time significantly reduce the quality. For a trade-off, we set λ to 0.5.

Locations to Insert the Orthogonal Noise Matrix. In Section 4, we have mentioned three places to insert the orthogonal noise matrix in Eq. (6), i.e., between $D_s^{\frac{1}{2}}$ and E_s^T , between E_s^T and \hat{F}_c , and on the right side of \hat{F}_c . We conduct the same experiments for each of them and find that there is no difference in qualitative comparisons. But in quantitative comparisons, e.g., run-time and computation requirements, they are obviously different. This is mainly due to the different computation of matrix multiplication caused by the different size of noise matrix. As we analyzed earlier in Section 4, when we insert the orthogonal noise matrix Z between $D_s^{\frac{1}{2}}$ and E_s^T , the size of Z is only $(C - k) \times (C - k)$,

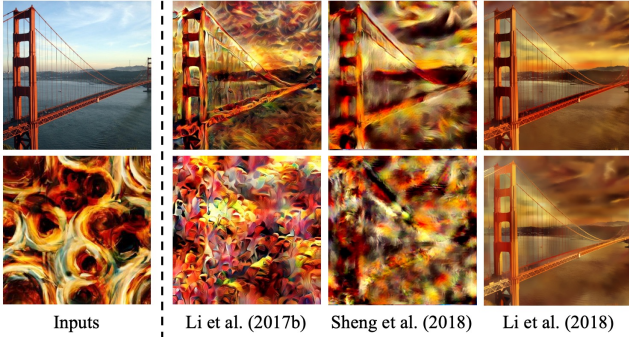


Figure 6: Orthogonal noise matrix vs. Random noise matrix. The first column shows the input content (top) and style (bottom) images. The right three columns show the results obtained by using the orthogonal noise matrix (top) and random noise matrix (bottom) to perturb the methods (Li et al. 2017b; Sheng et al. 2018; Li et al. 2018), respectively.

where C is the number of channels and k is the number of small singular values in $D_s^{\frac{1}{2}}$. For the other two cases, since the shapes of E_s^T and \hat{F}_c are $(C - k) \times C$ and $C \times H_c W_c$, respectively (where H_c, W_c are the height and width of the content feature), the size of Z should be $C \times C$ if we insert it between E_s^T and \hat{F}_c , and $H_c W_c \times H_c W_c$ if we insert it on the right side of \hat{F}_c . Generally, for the deepest level, $C - k < C < H_c W_c$. So we eventually insert Z between $D_s^{\frac{1}{2}}$ and E_s^T since this may consume the least computation and run-time.

Orthogonal Noise Matrix versus Random Noise Matrix. To verify the importance and necessity of the orthogonal noise matrix in our deep feature perturbation, we compare it with the original random noise matrix. Similar to previous experiments, we replace the deepest-level WCT in (Li et al. 2017b) and (Li et al. 2018) with our PWCT, the diversity hyperparameter λ is set to 1. And we replace the single-level WCT in (Sheng et al. 2018) with our PWCT, the diversity hyperparameter λ is set to 0.5. The results are shown in Fig. 6, as we can see, using original random noise matrix produces low quality results (bottom row). The results obtained by (Li et al. 2017b) and (Sheng et al. 2018) are just like combinations of texture and noise, which drown out the content information (see column 2 and 3 in bottom row). Compared with the former two, (Li et al. 2018) can maintain the content information as much as possible even with the original random noise perturbation (see the last column in bottom row). This is because it consists of two steps, and the second step removes noticeable artifacts to maintain the structure of the content image. But as we can see, the quality is still significantly reduced.

5.3 Comparisons

In this section, we incorporate our DFP into methods (Li et al. 2017b; Sheng et al. 2018; Li et al. 2018) and compare them with other diversified style transfer methods from both qualitative and quantitative aspects. Since method (Ulyanov,

Table 2: Quantitative comparisons of different methods. We measure diversity using average Pixel distance and LPIPS distance (Zhang et al. 2018).

	Pixel Distance	LPIPS Distance
(Li et al. 2017a)	0.080	0.175
(Li et al. 2017b)	0.000	0.000
(Sheng et al. 2018)	0.000	0.000
(Li et al. 2018)	0.000	0.000
(Li et al. 2017b) + our DFP	0.124	0.372
(Sheng et al. 2018) + our DFP	0.102	0.264
(Li et al. 2018) + our DFP	0.091	0.203

Vedaldi, and Lempitsky 2017) does not release pre-trained model or provide available codes to get diverse results, we only compare with method (Li et al. 2017a) and our base-lines. For method (Li et al. 2017a), we directly use its released pre-trained model and default settings. For ours, the settings are the same as those in previous experiments.

Qualitative Comparisons. We show qualitative comparison results in Fig. 7. We observe that (Li et al. 2017a) only produces subtle diversity (e.g., slight changes in shadows on cheeks), which does not contain any meaningful variation. By contrast, for the methods with our DFP, the results show a distinct diversity. Compared with the original outputs, the results obtained by incorporating our DFP have almost no quality degradation. More results can be found in our supplementary material.

Quantitative Comparisons. We compute the average distance of sample pairs in pixel space and deep feature space to measure the diversity, respectively. For each method, we use 6 content images and 6 style images to get 36 different combinations, and for each combination, we obtain 20 outputs. There are totally 6840 pairs (each pair has the same content and style) of outputs generated by each method, we compute the average distance between them.

In pixel space, we directly compute the average pixel distance in RGB channels, which can be formulated as follows:

$$Diff = \frac{\|P_1 - P_2\|_1}{W \times H \times 255 \times 3}, \quad (10)$$

where P_1 and P_2 denote the image pair to compute the distance. W and H are their width and height (they should have the same resolution).

In deep feature space, we use the LPIPS (Learned Perceptual Image Patch Similarity) metric proposed by Zhang et al. (2018). It computes distance in AlexNet (Krizhevsky 2014) feature space (*conv1_5*, pretrained on Imagenet (Russakovsky et al. 2015)), with linear weights to better match human perceptual judgments.

As shown in Table 2, (Li et al. 2017a) produces low diversity scores in both Pixel and LPIPS distance. Without our modification, the original methods (Li et al. 2017b; Sheng et al. 2018; Li et al. 2018) could not produce diverse results. By incorporating our DFP, these methods can obtain much higher diversity scores. Note that since the diversity

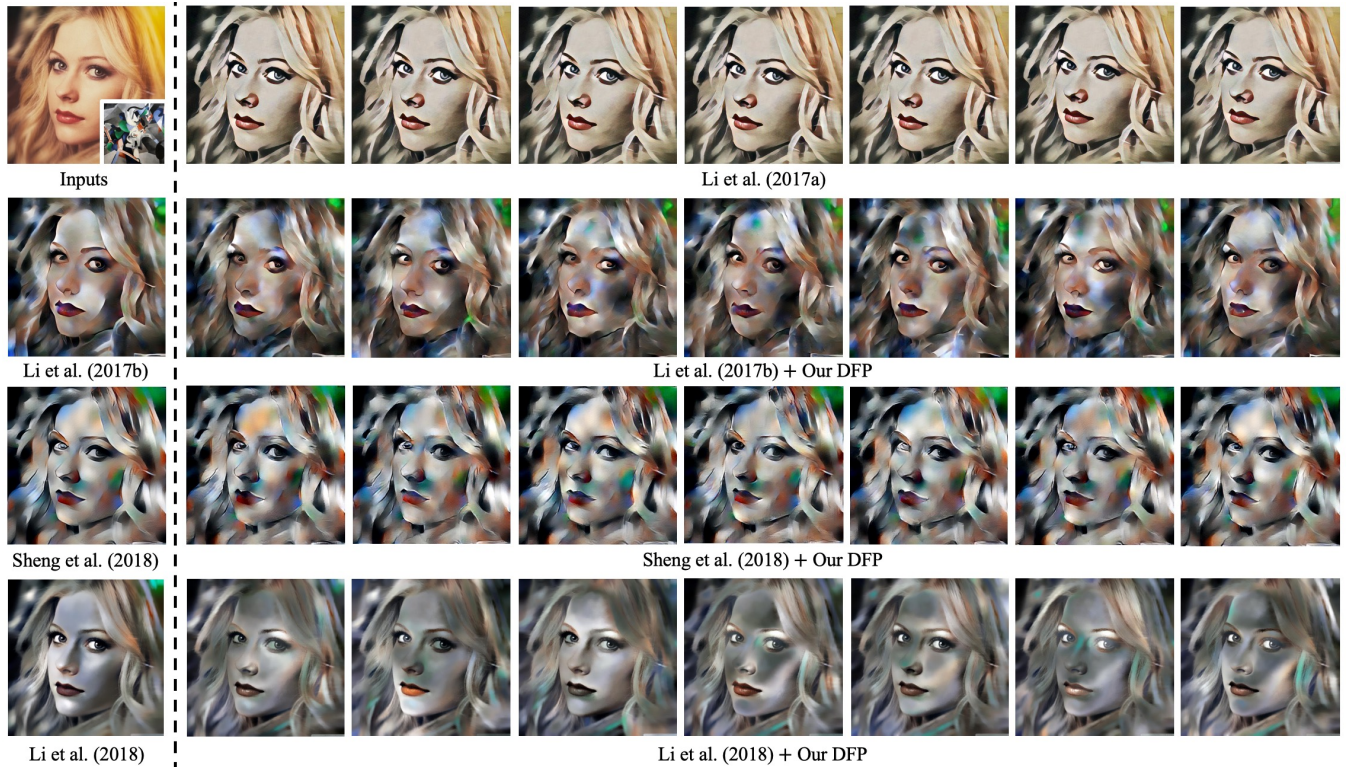


Figure 7: Qualitative comparisons of different methods. The first column (from top to bottom) shows inputs and original outputs of (Li et al. 2017b; Sheng et al. 2018; Li et al. 2018). The other columns (from top to bottom) show diverse outputs of (Li et al. 2017a) and (Li et al. 2017b; Sheng et al. 2018; Li et al. 2018) (with our DFP).

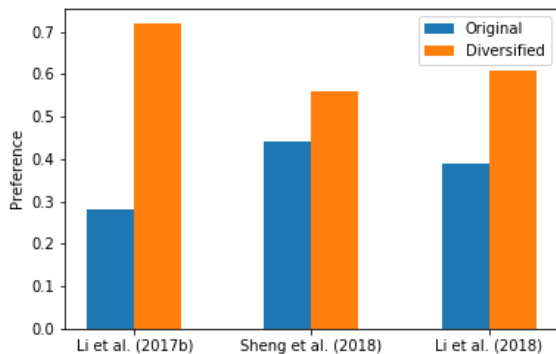


Figure 8: User study results.

hyperparameter λ of method (Sheng et al. 2018) (+ our DFP) is only set to 0.5, and method (Li et al. 2018) (+ our DFP) still contains a smoothing step to remove detailed effects, their diversity scores are lower than those of method (Li et al. 2017b) (+ our DFP).

User Study. Diverse outputs could provide users with more choices according to their preference. To justify the superiority of our diversified methods, we conduct several new

user studies for the pairs of original methods (Li et al. 2017b; Sheng et al. 2018; Li et al. 2018) and our corresponding diversified methods, respectively. For each pair, we show participants 100 groups (each group contains one output of the original method and one random output of our corresponding diversified method, note that these two outputs should have the same content and style) and ask them to select their preferred one in each group. We finally collect totally 3000 votes from 30 subjects for each method pair and demonstrate the preference results in Fig. 8. The studies show that our diversified methods receive more votes than the original methods, which means that our diversified methods can help users obtain more satisfactory results.

6 Conclusion

In this work, we introduce deep feature perturbation into the whitening and coloring transforms (WCT) to achieve diversified arbitrary style transfer. By incorporating our method, many existing WCT-based methods can be empowered to produce diverse results. Experimental results demonstrate that our approach can greatly increase the diversity while maintaining the quality of stylization. And several new user studies show that users could obtain more satisfactory results through the diversified methods based on our approach.

References

- Champanand, A. J. 2016. Semantic style transfer and turning two-bit doodles into fine artworks. *arXiv preprint arXiv:1603.01768*.
- Chen, T. Q., and Schmidt, M. 2016. Fast patch-based style transfer of arbitrary style. *arXiv preprint arXiv:1612.04337*.
- Chen, D.; Yuan, L.; Liao, J.; Yu, N.; and Hua, G. 2017. Stylebank: An explicit representation for neural image style transfer. In *Proceedings of the IEEE conference on computer vision and pattern recognition*, 1897–1906.
- Dumoulin, V.; Shlens, J.; and Kudlur, M. 2017. A learned representation for artistic style. *Proc. of ICLR*.
- Gatys, L. A.; Ecker, A. S.; Bethge, M.; Hertzmann, A.; and Shechtman, E. 2017. Controlling perceptual factors in neural style transfer. In *Proceedings of the IEEE Conference on Computer Vision and Pattern Recognition*, 3985–3993.
- Gatys, L.; Ecker, A. S.; and Bethge, M. 2015a. Texture synthesis using convolutional neural networks. In *Advances in Neural Information Processing Systems*, 262–270.
- Gatys, L. A.; Ecker, A. S.; and Bethge, M. 2015b. A neural algorithm of artistic style. *arXiv preprint arXiv:1508.06576*.
- Gatys, L. A.; Ecker, A. S.; and Bethge, M. 2016. Image style transfer using convolutional neural networks. In *Proceedings of the IEEE Conference on Computer Vision and Pattern Recognition*, 2414–2423.
- Gu, S.; Chen, C.; Liao, J.; and Yuan, L. 2018. Arbitrary style transfer with deep feature reshuffle. In *Proceedings of the IEEE Conference on Computer Vision and Pattern Recognition*, 8222–8231.
- Huang, X., and Belongie, S. 2017. Arbitrary style transfer in real-time with adaptive instance normalization. In *Proceedings of the IEEE International Conference on Computer Vision*, 1501–1510.
- Johnson, J.; Alahi, A.; and Fei-Fei, L. 2016. Perceptual losses for real-time style transfer and super-resolution. In *European Conference on Computer Vision*, 694–711. Springer.
- Julesz, B. 1981. Textons, the elements of texture perception, and their interactions. *Nature* 290(5802):91.
- Krizhevsky, A. 2014. One weird trick for parallelizing convolutional neural networks. *arXiv preprint arXiv:1404.5997*.
- Li, C., and Wand, M. 2016a. Combining markov random fields and convolutional neural networks for image synthesis. In *Proceedings of the IEEE Conference on Computer Vision and Pattern Recognition*, 2479–2486.
- Li, C., and Wand, M. 2016b. Precomputed real-time texture synthesis with markovian generative adversarial networks. In *European Conference on Computer Vision*, 702–716. Springer.
- Li, Y.; Fang, C.; Yang, J.; Wang, Z.; Lu, X.; and Yang, M.-H. 2017a. Diversified texture synthesis with feed-forward networks. In *Proceedings of the IEEE Conference on Computer Vision and Pattern Recognition*.
- Li, Y.; Fang, C.; Yang, J.; Wang, Z.; Lu, X.; and Yang, M.-H. 2017b. Universal style transfer via feature transforms. In *Advances in Neural Information Processing Systems*, 386–396.
- Li, Y.; Liu, M.-Y.; Li, X.; Yang, M.-H.; and Kautz, J. 2018. A closed-form solution to photorealistic image stylization. In *Proceedings of the European Conference on Computer Vision (ECCV)*, 453–468.
- Li, X.; Liu, S.; Kautz, J.; and Yang, M.-H. 2019. Learning linear transformations for fast arbitrary style transfer. In *Proceedings of the IEEE Conference on Computer Vision and Pattern Recognition*.
- Liao, J.; Yao, Y.; Yuan, L.; Hua, G.; and Kang, S. B. 2017. Visual attribute transfer through deep image analogy. *ACM Trans. Graph.*
- Luan, F.; Paris, S.; Shechtman, E.; and Bala, K. 2017. Deep photo style transfer. In *Proceedings of the IEEE Conference on Computer Vision and Pattern Recognition*, 4990–4998.
- Russakovsky, O.; Deng, J.; Su, H.; Krause, J.; Satheesh, S.; Ma, S.; Huang, Z.; Karpathy, A.; Khosla, A.; Bernstein, M.; et al. 2015. Imagenet large scale visual recognition challenge. *International journal of computer vision* 115(3):211–252.
- Sheng, L.; Lin, Z.; Shao, J.; and Wang, X. 2018. Avatar-net: Multi-scale zero-shot style transfer by feature decoration. In *Proceedings of the IEEE Conference on Computer Vision and Pattern Recognition*, 8242–8250.
- Simonyan, K., and Zisserman, A. 2014. Very deep convolutional networks for large-scale image recognition. *arXiv preprint arXiv:1409.1556*.
- Ulyanov, D.; Lebedev, V.; Vedaldi, A.; and Lempitsky, V. S. 2016. Texture networks: Feed-forward synthesis of textures and stylized images. In *ICML*, 1349–1357.
- Ulyanov, D.; Vedaldi, A.; and Lempitsky, V. 2017. Improved texture networks: Maximizing quality and diversity in feed-forward stylization and texture synthesis. In *Proceedings of the IEEE Conference on Computer Vision and Pattern Recognition*, volume 1, 6.
- Wang, X.; Oxholm, G.; Zhang, D.; and Wang, Y.-F. 2017. Multimodal transfer: A hierarchical deep convolutional neural network for fast artistic style transfer. In *Proceedings of the IEEE Conference on Computer Vision and Pattern Recognition*, volume 2, 7.
- Zhang, H., and Dana, K. 2018. Multi-style generative network for real-time transfer. In *European Conference on Computer Vision*, 349–365. Springer.
- Zhang, R.; Isola, P.; Efros, A. A.; Shechtman, E.; and Wang, O. 2018. The unreasonable effectiveness of deep features as a perceptual metric. In *Proceedings of the IEEE Conference on Computer Vision and Pattern Recognition*.
- Zhu, S. C.; Liu, X. W.; and Wu, Y. N. 2000. Exploring texture ensembles by efficient markov chain monte carlo-toward a “trichromacy” theory of texture. *IEEE Transactions on Pattern Analysis and Machine Intelligence* 22(6):554–569.